Determining the hotspot geometry with HERA data

Tobias Toll, Nahid Vasim
Indian Institute of Technology Delhi

arXiv:2607.14955

Exclusive diffraction in the Dipole Model

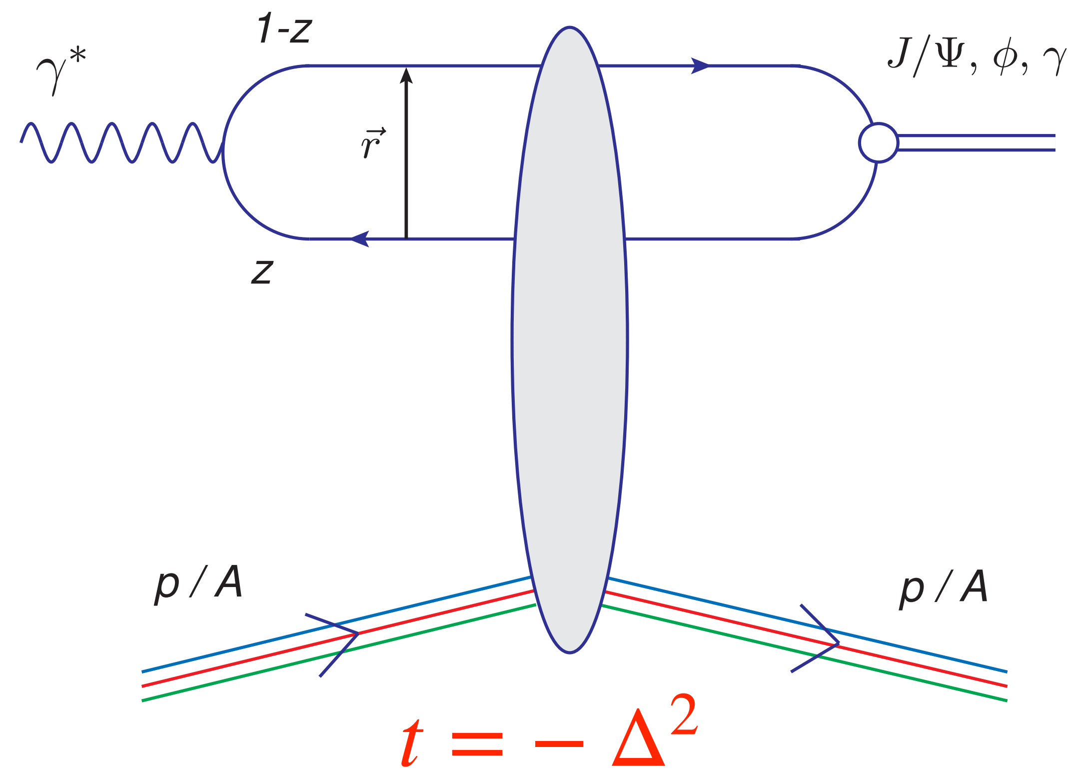

$$\frac{d\sigma^{\gamma^* p \to Vp}}{dt} = \frac{1}{16\pi} \left\langle \left| \mathcal{A}_{T,L}^{\gamma^* p \to Vp} \right|^2 \right\rangle_{\text{initial state}}$$

$$\mathcal{A}_{T,L}^{\gamma^* p \to Vp}(x_{I\!P}, Q^2, \Delta) = i \int 2\pi r dr \int \frac{dz}{4\pi} \int d^2\vec{b} \left(\Psi_V^* \Psi\right)(r,z) J_0([1-z]r\Delta) e^{-\vec{b}\cdot\vec{\Delta}} \frac{d\sigma_{q\bar{q}}}{d^2\vec{b}}(x_{I\!P}, r, \vec{b})$$

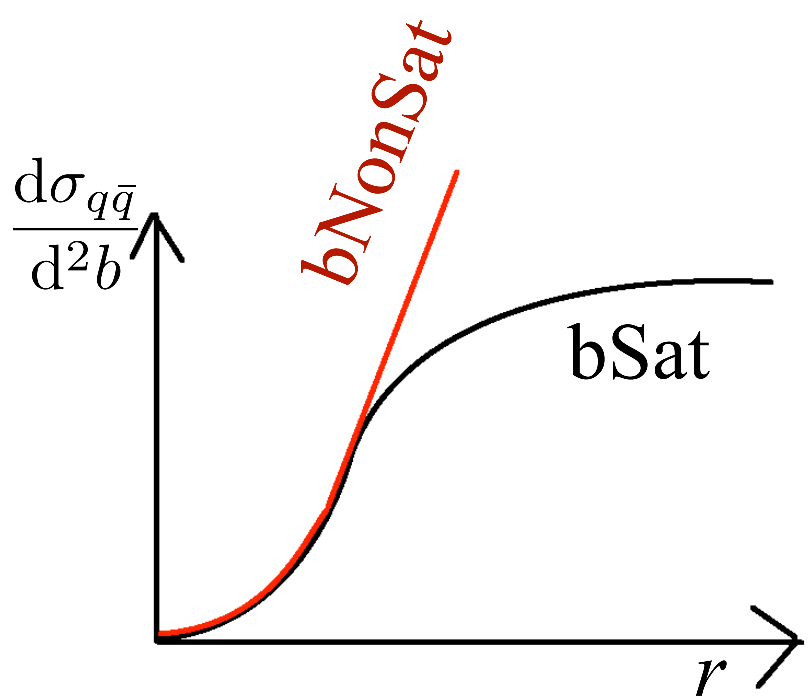

$$\frac{d\sigma_{q\bar{q}}}{d^2\mathbf{b}} = 2\left[1 - \exp\left(-\frac{\pi^2}{2N_c} r^2 \alpha_s(\mu^2) x g(x, \mu^2) T(b)\right)\right]$$

$$\frac{d\sigma_{q\bar{q}}^{\text{nosat}}}{d\mathbf{b}_2} = \frac{\pi^2}{N_C} r^2 \alpha_S(\mu^2) x g(x, \mu^2) T(b)$$

H. Kowalski, L. Motyka, G. Watt, Phys.Rev.D 74 (2006) 074016, arXiv: hep-ph/0606272

Exclusive diffraction in the Dipole Model

$$\frac{\mathrm{d}\sigma_{q\bar{q}}}{\mathrm{d}^2\mathbf{b}} = 2\left[1 - \exp\left(-\frac{\pi^2}{2N_c} r^2 \alpha_s(\mu^2) xg(x,\mu^2) T(b)\right)\right]$$

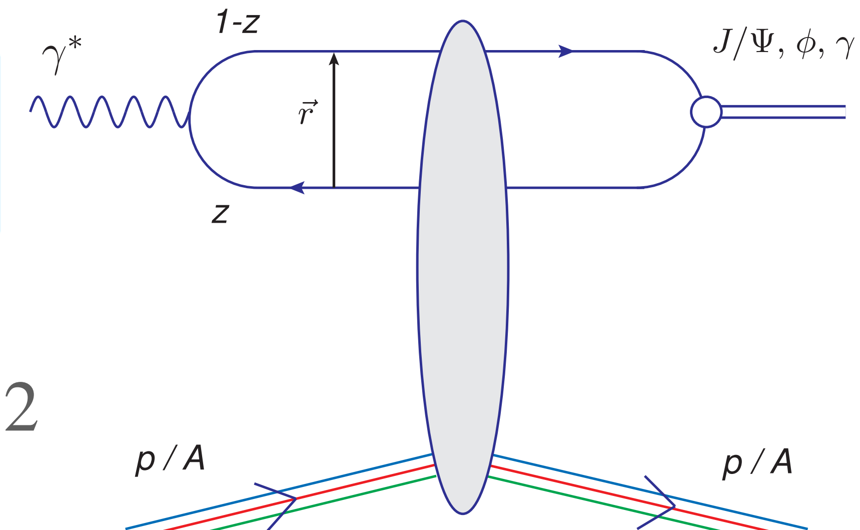

$$T_p(b) = \frac{1}{2\pi B_G} e^{-\frac{b^2}{2B_G}} \quad B_G = 4\ \mathrm{GeV}^{-2}$$

$$t = -\Delta^2$$

$$\frac{\mathrm{d}\sigma}{\mathrm{d}t} \propto e^{-Bt}$$

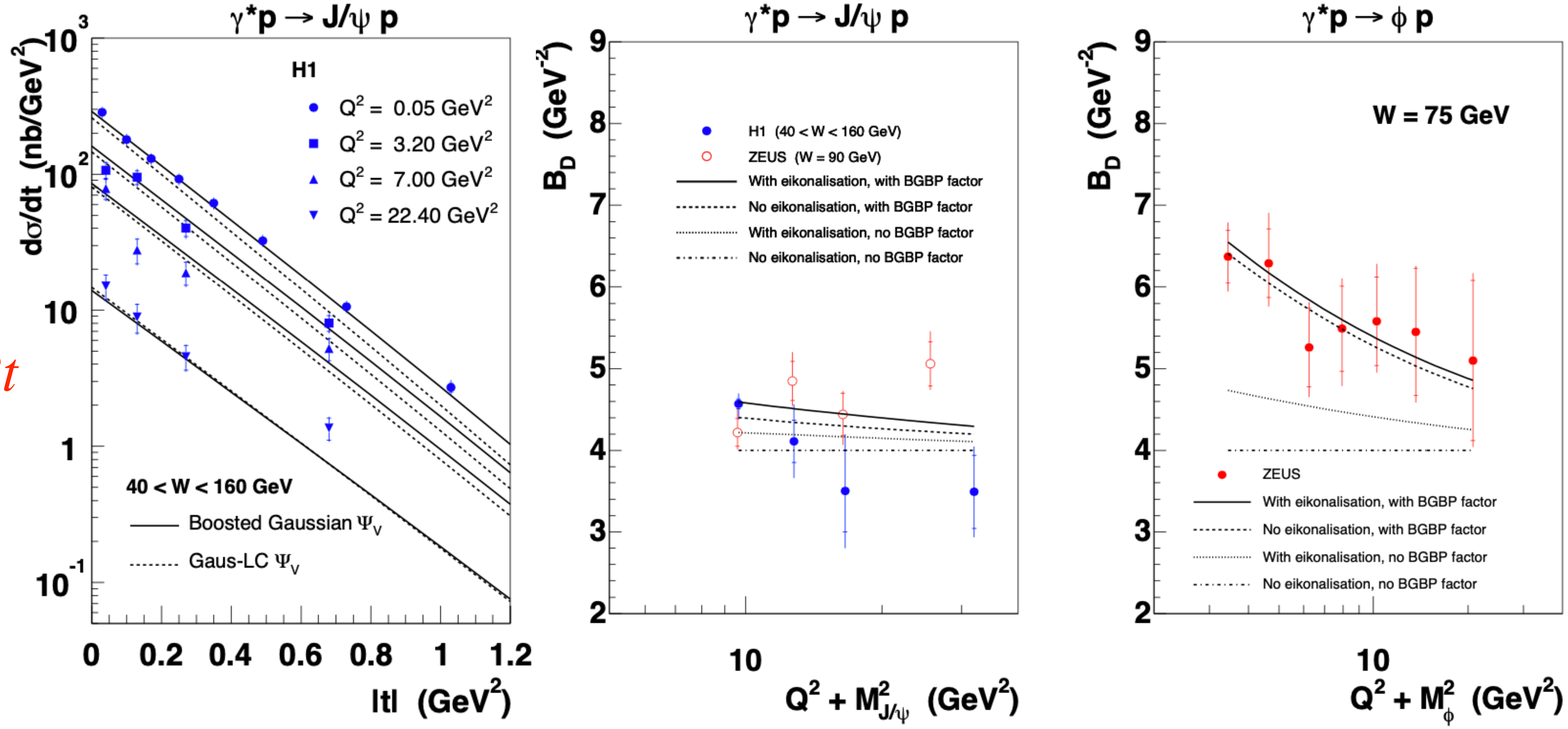

Incoherent Scattering

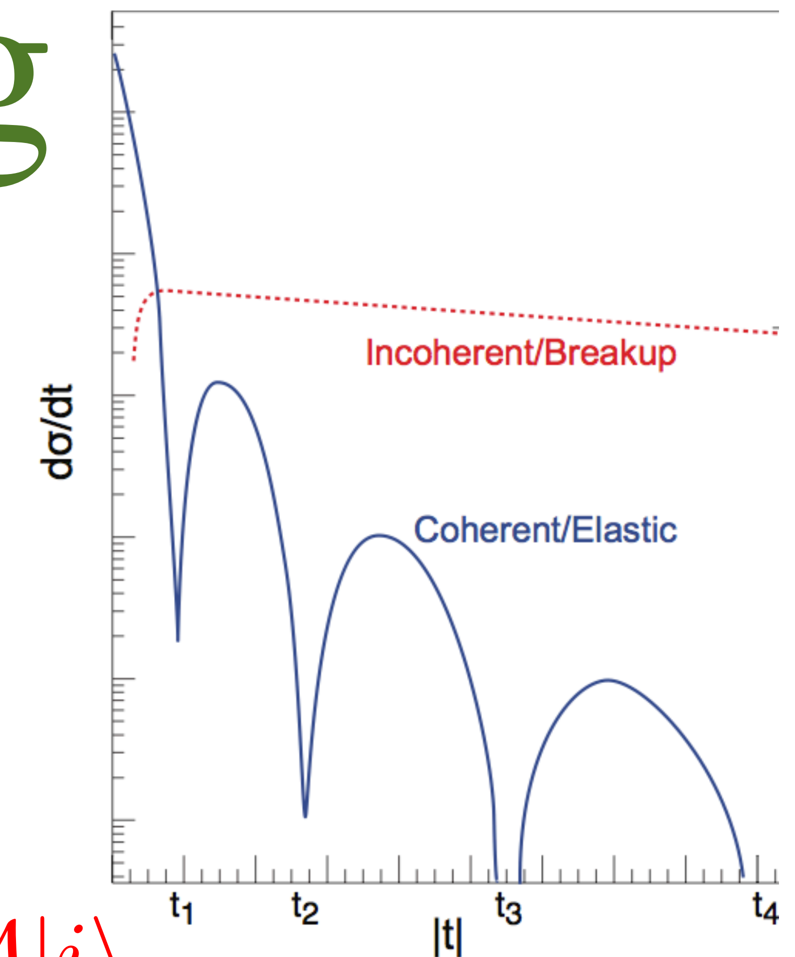

Good, Walker:

Nucleus dissociates ($f \neq i$):

$$\sigma_{\text{incoherent}} \propto \sum_{f\neq i} \langle i|\mathcal{A}|f\rangle^\dagger \langle f|\mathcal{A}|i\rangle$$

$$= \sum_f \langle i|\mathcal{A}\overbrace{|f\rangle^\dagger \langle f|}^{\text{complete set}}\mathcal{A}|i\rangle - \langle i|\mathcal{A}|i\rangle^\dagger \langle i|\mathcal{A}|i\rangle$$

$$= \left\langle i \left| |\mathcal{A}|^2 \right| i \right\rangle - |\langle i|\mathcal{A}|i\rangle|^2 = \left\langle |\mathcal{A}|^2 \right\rangle - |\langle \mathcal{A} \rangle|^2$$

The incoherent CS is the variance of the amplitude!!

$$\frac{d\sigma_{\text{total}}}{dt} = \frac{1}{16\pi} \left\langle |\mathcal{A}|^2 \right\rangle \qquad \frac{d\sigma_{\text{coherent}}}{dt} = \frac{1}{16\pi} |\langle \mathcal{A} \rangle|^2$$

Incoherent Scattering in *ep*

$$\frac{\mathrm{d}\sigma_{q\bar{q}}}{\mathrm{d}^2\mathbf{b}} = 2\left[1 - \exp\left(-\frac{\pi^2}{2N_c} r^2 \alpha_s(\mu^2) xg(x,\mu^2) T(b)\right)\right]$$

$$xg(x,\mu_0^2) = A_g x^{-\lambda_g}(1-x)^6$$

$$\mu^2 = \mu_0^2 + \frac{C}{r^2}$$

$$T_p(b) = \frac{1}{2\pi B_G} e^{-\frac{b^2}{2B_G}}$$

$$\downarrow$$

$$T_p(b) = \frac{1}{2\pi N_q B_q} \sum_{i=1}^{N_q} e^{-\frac{(\vec{b}-\vec{b}_i)^2}{2B_q}}$$

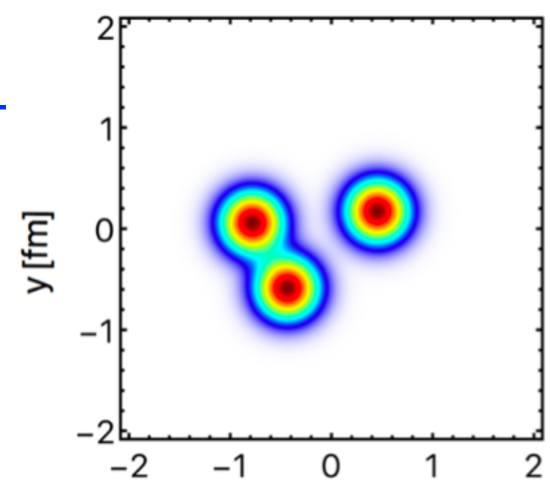

$\vec{b}_i$ with a Gaussian distribution of width B_{qc}

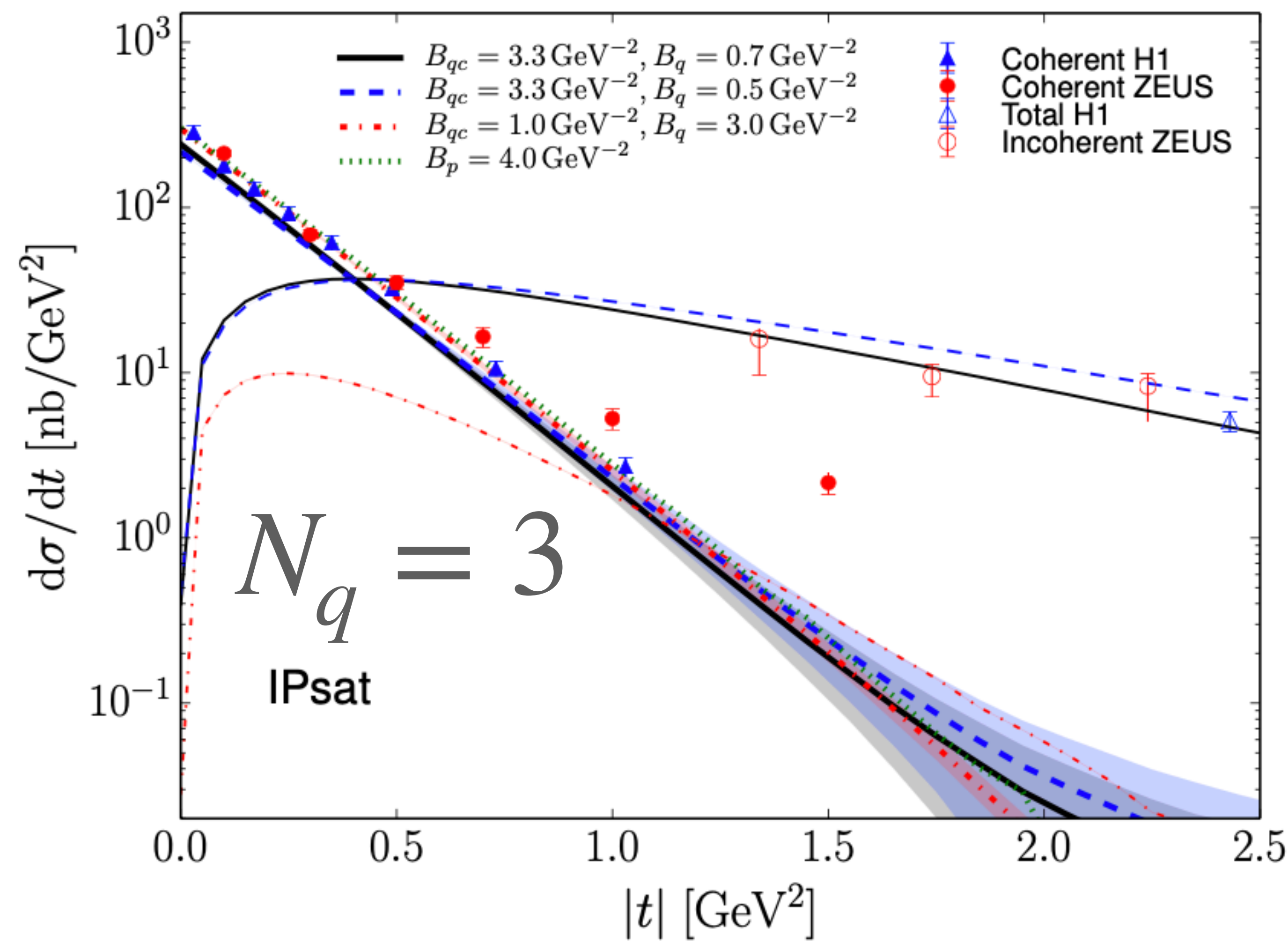

H. Mäntysaari and B. Schenke Phys. Rev. Lett., 117(5):052301, 2016.

Also: large scale (small $|t|$) saturation scale fluctuations. Affects small $|t|$, one more parameter.

Incoherent Scattering in *ep*

$$\frac{\mathrm{d}\sigma_{q\bar{q}}^{\mathrm{nosat}}}{\mathrm{d}\mathbf{b}} = \frac{\pi^2}{N_C} r^2 \alpha_S(\mu^2) xg(x,\mu^2) T(b)$$

$$xg(x,\mu_0^2) = A_g x^{-\lambda_g}(1-x)^6$$

$$\mu^2 = \mu_0^2 + \frac{C}{r^2}$$

$$T_p(b) = \frac{1}{2\pi B_G} e^{-\frac{b^2}{2B_G}}$$

$$\downarrow$$

$$T_p(b) = \frac{1}{2\pi N_q B_q} \sum_{i=1}^{N_q} e^{-\frac{(\vec{b}-\vec{b}_i)^2}{2B_q}}$$

$\vec{b}_i$ with a Gaussian distribution of width B_{qc}

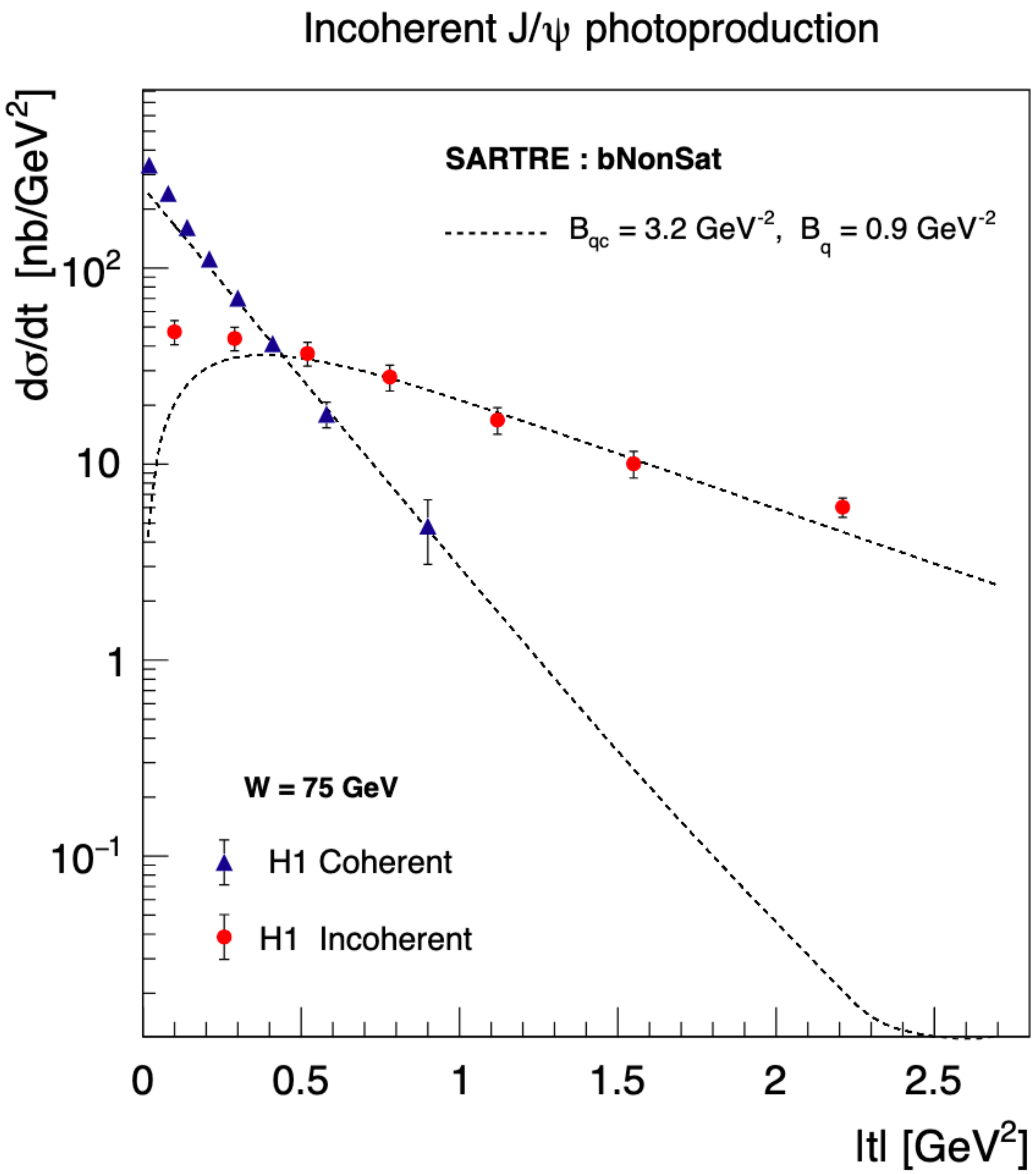

Arjun Kumar, TT, Eur.Phys.J.C 82 (2022) 9, 837, arXiv: 2106.12855

Incoherent Scattering in *ep*

$$\frac{d\sigma_{q\bar{q}}}{d^2\mathbf{b}} = 2\left[1 - \exp\left(-\frac{\pi^2}{2N_c} r^2 \alpha_s(\mu^2) x g(x, \mu^2) T(b)\right)\right]$$

$$\frac{d\sigma^{\mathrm{nosat}}_{\mathrm{q\bar{q}}}}{d\mathbf{b}} = \frac{\pi^2}{N_C} r^2 \alpha_S(\mu^2) x g(x, \mu^2) T(b)$$

$$xg(x, \mu_0^2) = A_g x^{-\lambda_g}(1-x)^6$$

$$\mu^2 = \mu_0^2 + \frac{C}{r^2}$$

For bNonSat, $\langle \mathscr{A} \rangle \propto \langle T(b) \rangle$

Modified profile:

$$T_{qc}(b) = \frac{1}{2\pi B_{qc}} \frac{1}{\exp\left(\frac{b^2}{2B_{qc}}\right) - S_g}$$

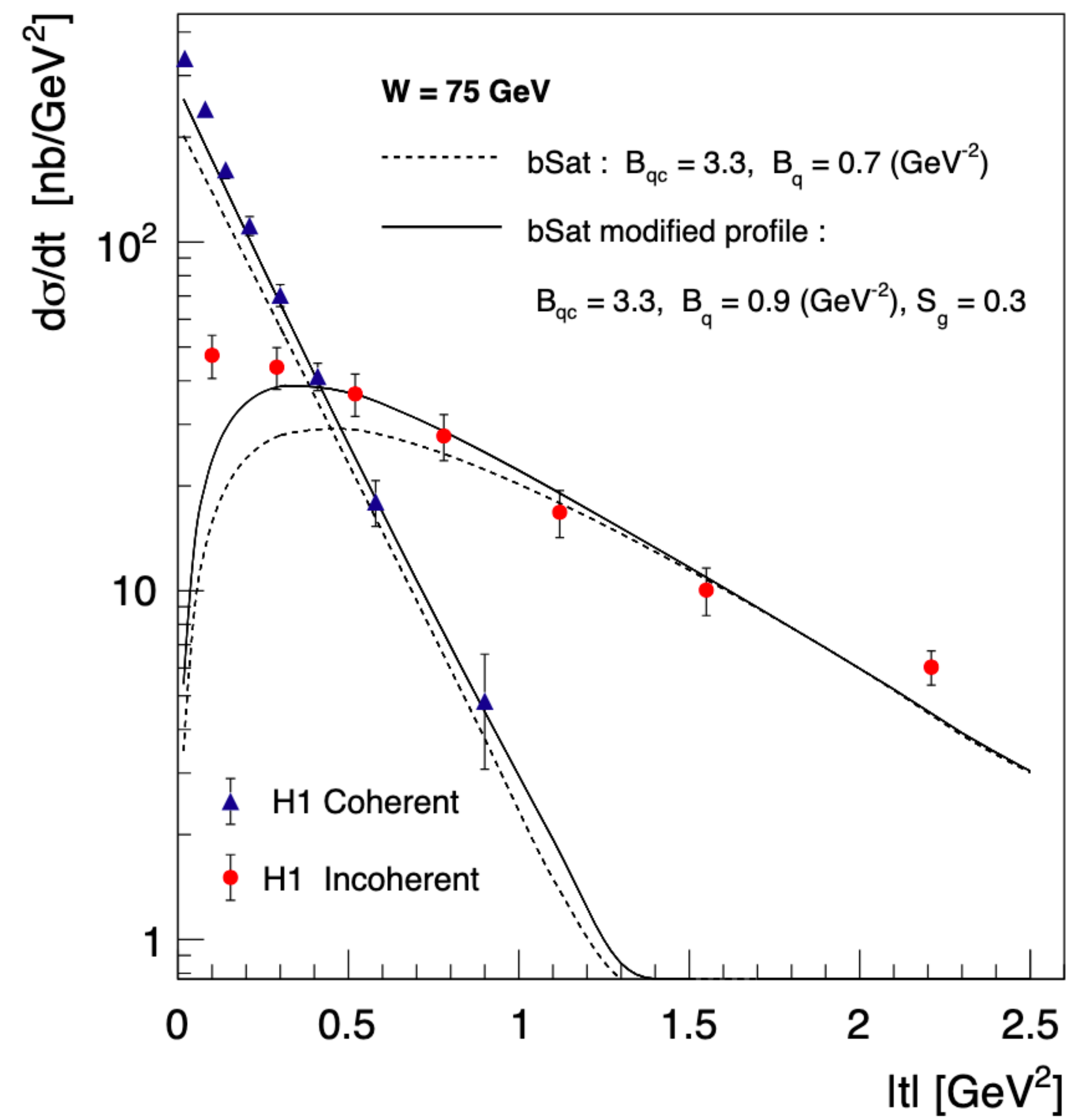

$\vec{b}_i$ with a Gaussian distribution of width B_{qc}

Arjun Kumar, TT, Eur.Phys.J.C 82 (2022) 9, 837, arXiv: 2106.12855

Larger $|t|$?

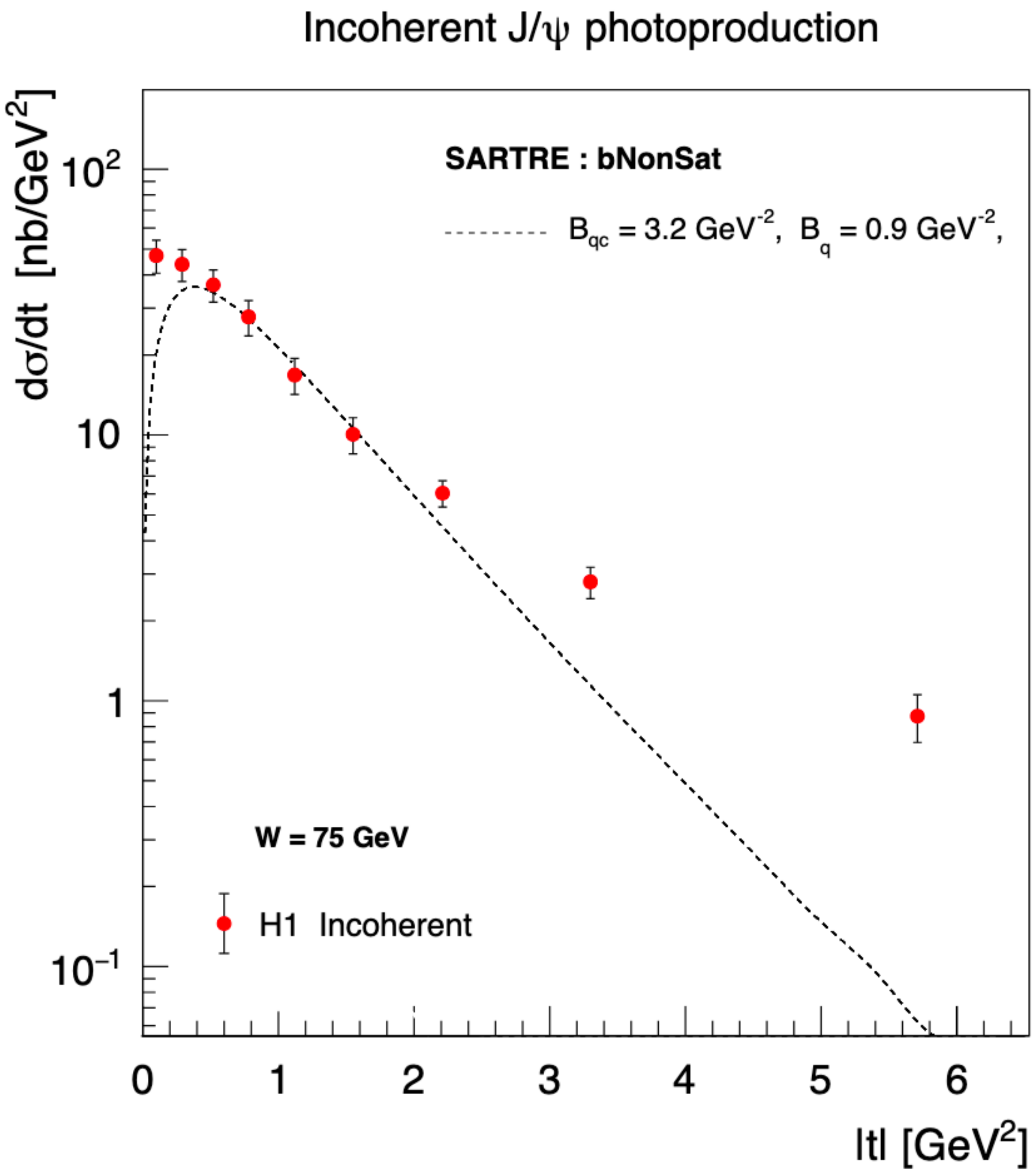

Appears to be two slopes in the data:
One for $0.5 \leq |t| \leq 2$ GeV^2
Another for $|t| > 2$ GeV^2

Which hotspot substructure can reproduce the t-spectrum?

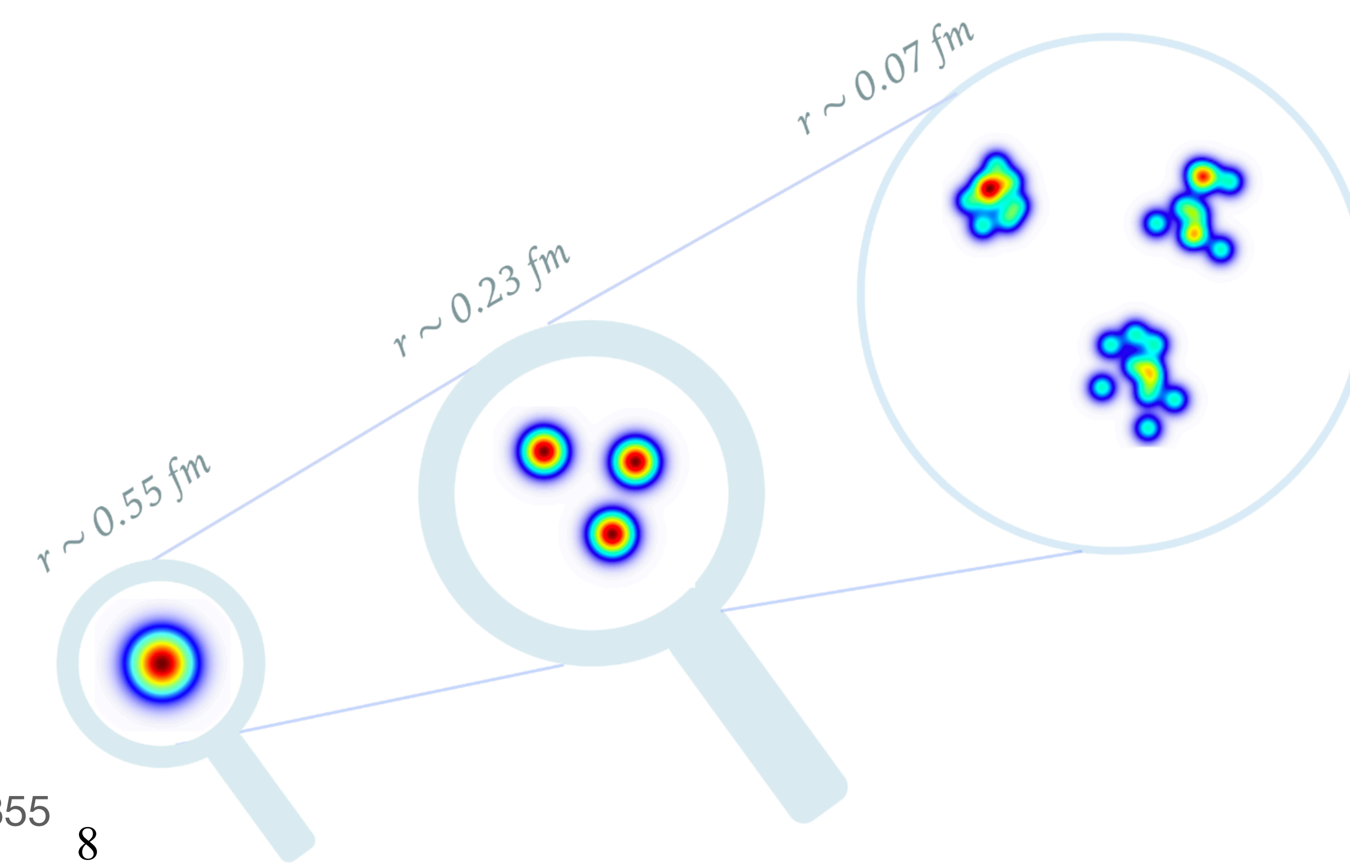

Arjun Kumar, TT, Eur.Phys.J.C 82 (2022) 9, 837, arXiv: 2106.12855

CGC calculations

S. Demirci, T. Lappi, S. Schlichting, Phys.Rev.D 106 (2022) 7, 074025

Non-relativistic limit

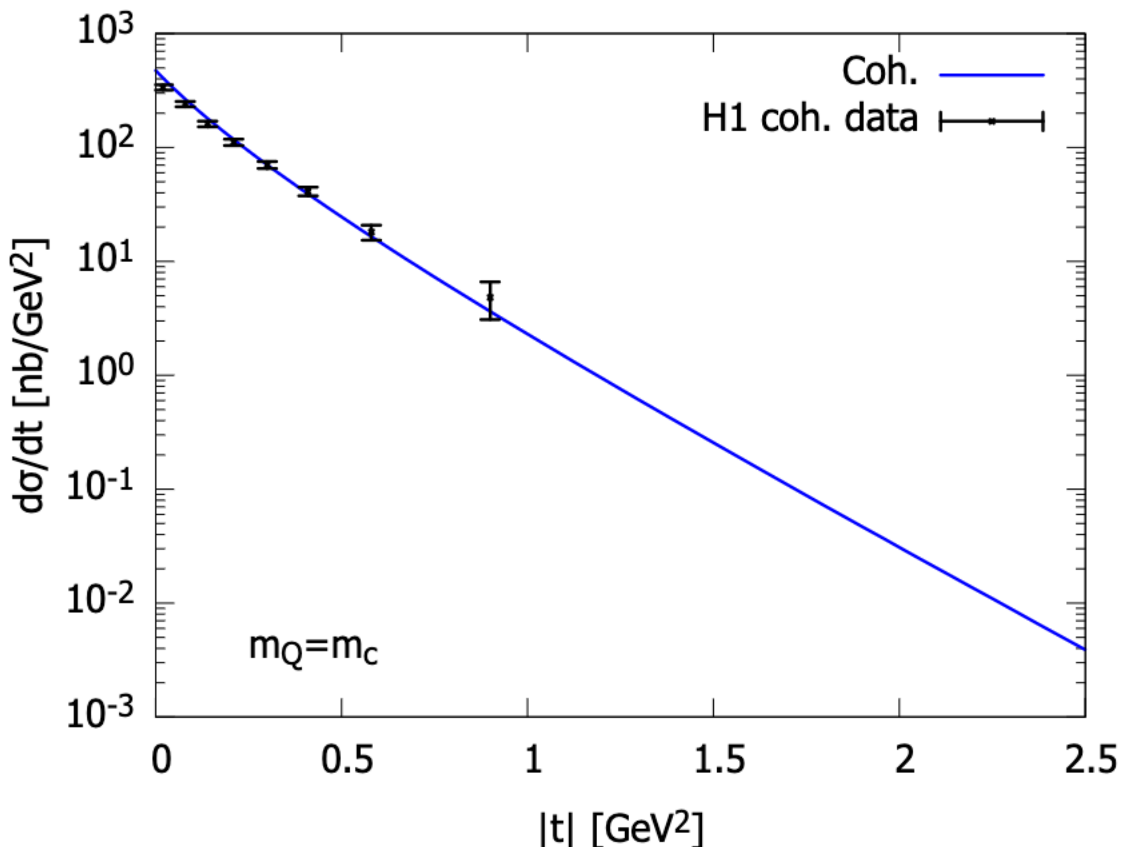

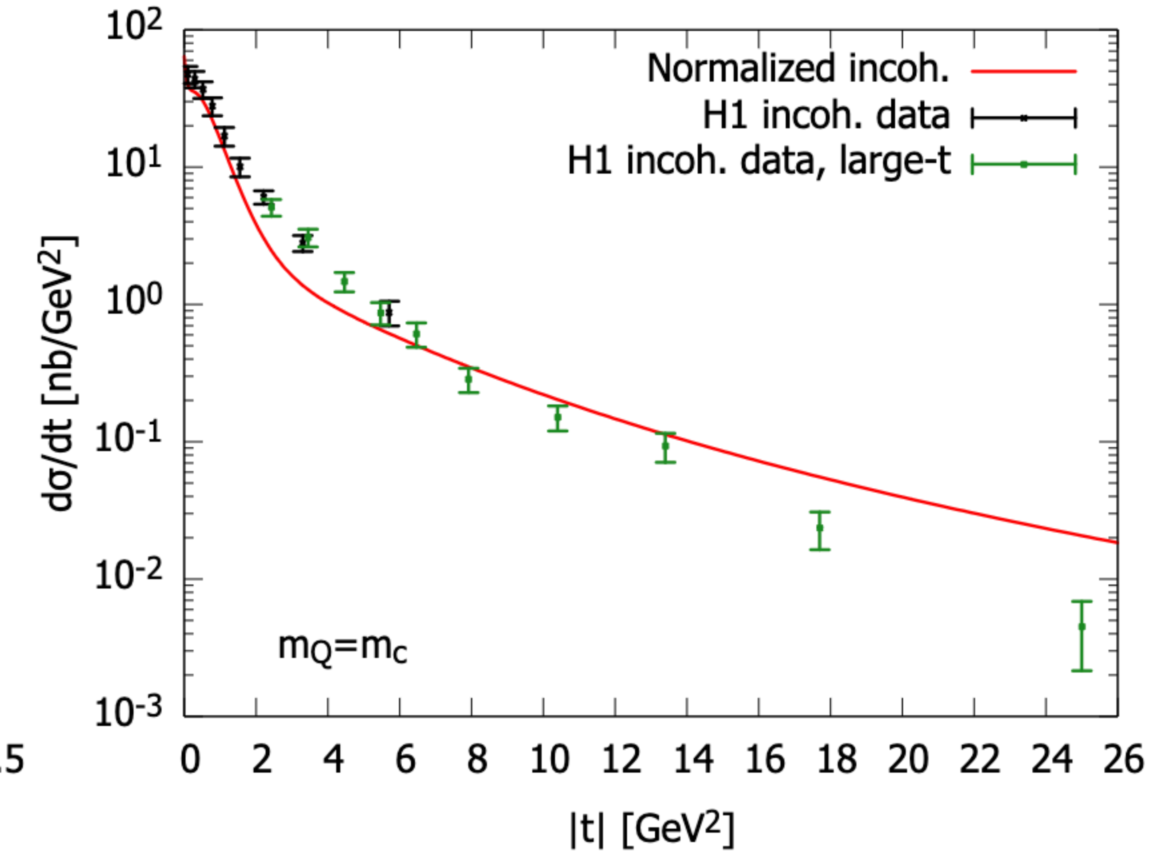

Wilson lines

$$\rho \to V(x) \to \mathcal{N}(x, Y) \to J/\psi$$

Fluctuating colour point sources

JIMWLK evolution

CGC calculations

A.D. Le, H. Mäntysaari, Phys.Rev.D 112 (2025) 11, 114006

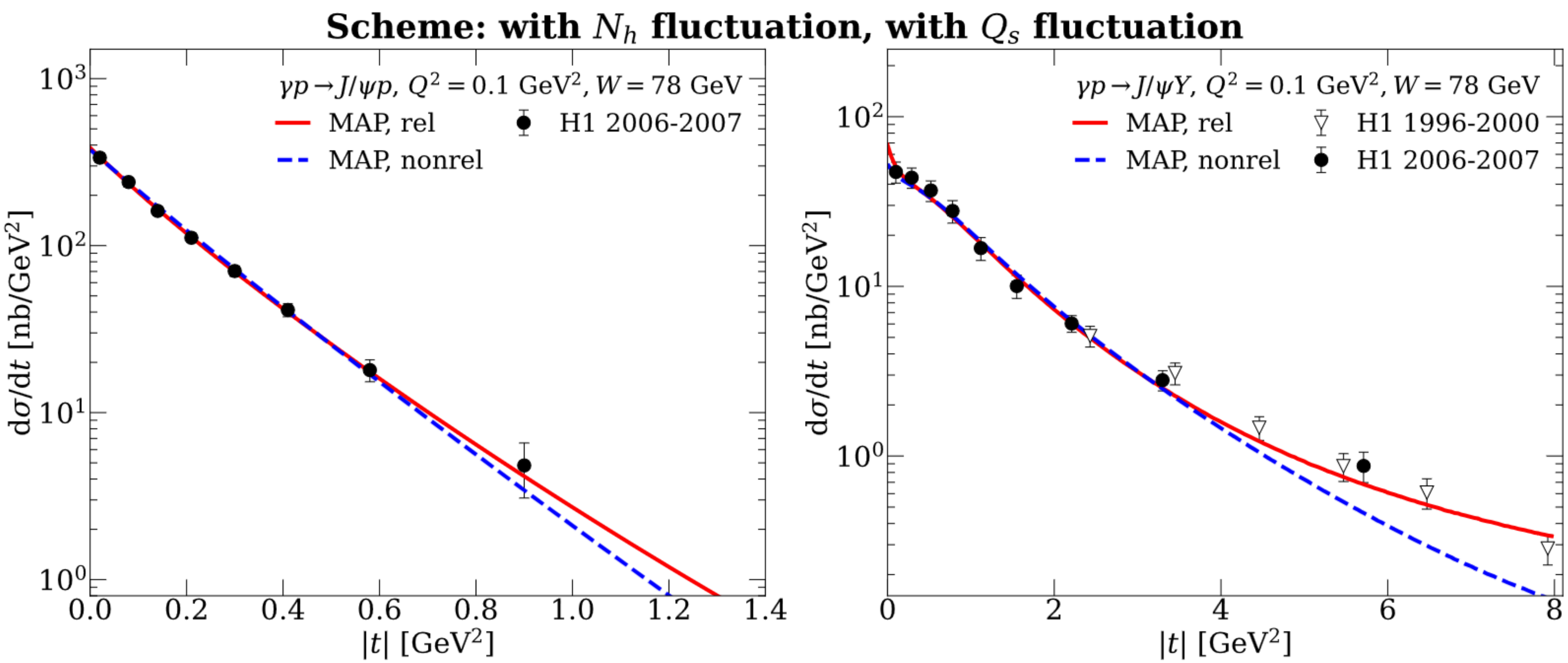

FIG. 10: Fit result compared to the H1 data [42, 68].

Wilson lines

$$\rho \to V(x) \to \mathcal{N}(x, Y) \to J/\psi$$

Fluctuating colour point sources JIMWLK evolution

Hotspot Evolution?

$$\frac{dP}{dt} = \frac{\alpha}{|t|}\frac{t - t_0}{t}\exp\left[-\alpha\left(\frac{t_0}{t} - \ln\frac{t_0}{t} - 1\right)\right]$$

$$\alpha = 18.5$$
$$t_0 = 1.1\ \mathrm{GeV}^2$$

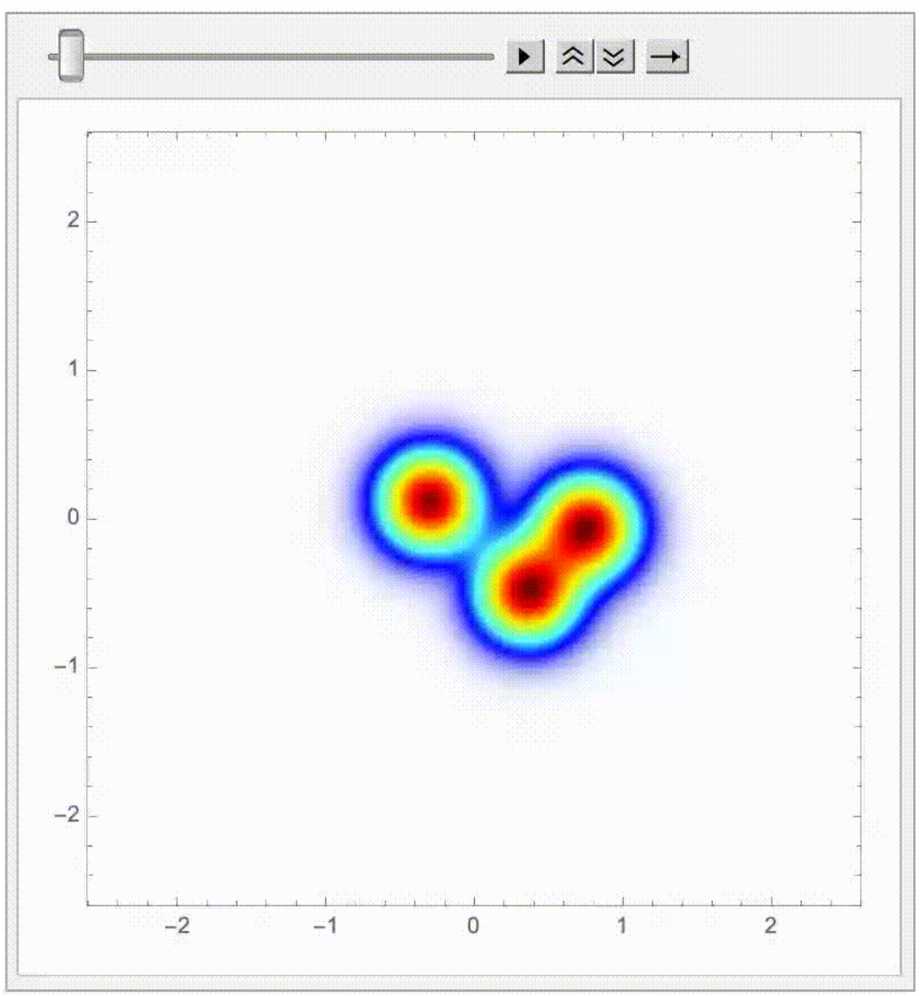

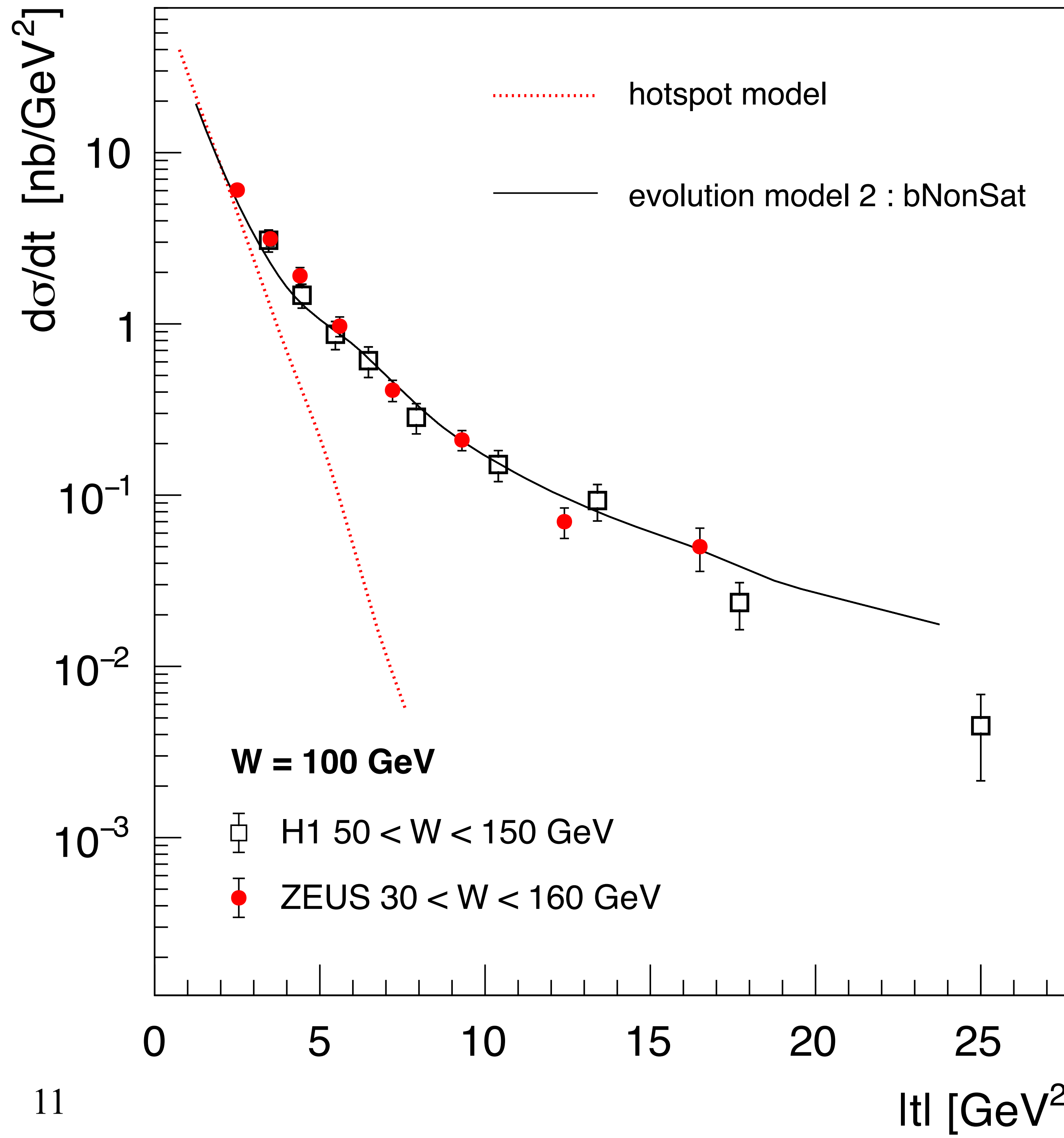

Analytical calculation of the Thickness function

Analytical calculation of the cross sections

IPnonsat (leading twist):

$$\mathscr{A}^{\gamma^* p}(x_P, \Delta) = \int_0^\infty \mathrm{d}r \int_0^1 \mathrm{d}z D_{rz}^{x_P} \int_0^\infty \mathrm{d}^2\vec{b} e^{-i\vec{\Delta}\vec{b}} T_p(\vec{b})$$

$$T_p(\vec{b}) = \frac{1}{N_{hs}} \sum_{i=1}^{N_{hs}} T_{hs}(\vec{b} - \vec{b}_i)$$

$\vec{b}_i$ from $T_c(\vec{b})$

$$D_{rz}^{x_P} = (\Psi^*\Psi_V)(r,z)\frac{r^2\pi^2}{2N_C}\alpha_S(\mu^2)x_P g(x_P,\mu^2)J_0\left((\frac{1}{2}-z)r\Delta\right)$$

$$\tilde{T}(\Delta) = \int_0^\infty \mathrm{d}^2\vec{b} e^{-i\vec{\Delta}\vec{b}} T_p(\vec{b}) = \frac{1}{N_{hs}} \sum_{i=1}^{N_{hs}} \int_0^\infty \mathrm{d}^2\vec{b} e^{-i\vec{\Delta}\cdot\vec{b}} T_{hs}(\vec{b} - \vec{b}_i) = \frac{\hat{T}(|t|)}{N_{hs}} \sum_{i=1}^{N_{hs}} e^{-i\vec{\Delta}\cdot\vec{b}}$$

Analytical calculation of the cross sections

IPnonsat (leading twist):

$$\tilde{T}(|t|) = \frac{\hat{T}(|t|)}{N_{hs}} \sum_{i=1}^{N_{hs}} e^{-i\vec{\Delta}\cdot\vec{b}}$$

$$\frac{d\sigma_{\text{coh.}}}{dt} \propto \left| \left\langle \tilde{T}(\vec{\Delta}) \right\rangle \right|^2$$

$$\frac{d\sigma_{\text{inc.}}}{dt} \propto \left\langle \left| \tilde{T}(\vec{\Delta}) \right|^2 \right\rangle - \left| \left\langle \tilde{T}(\vec{\Delta}) \right\rangle \right|^2$$

First moment:

Let $\phi(|t|) \equiv \left\langle e^{-i\vec{\Delta}\cdot\vec{b}} \right\rangle = \int d^2\vec{b}\, T_c(\vec{b}) e^{-i\vec{b}\vec{\Delta}} = e^{-B_{qc}|t|/2}$ Assuming Gaussian centres

$$\left\langle \tilde{T}(|t|) \right\rangle = \frac{\hat{T}(|t|)}{N_{hs}} \sum_{i=1}^{N_{hs}} \left\langle e^{i\vec{\Delta}\cdot\vec{b}} \right\rangle = \hat{T} e^{-B_{qc}|t|/2}$$

Assuming independent hotspots

Analytical calculation of the cross sections

IPnonsat (leading twist):

$$\frac{\mathrm{d}\sigma_{\mathrm{coh.}}}{\mathrm{d}t} \propto \left| \left\langle \tilde{T}(\vec{\Delta}) \right\rangle \right|^2$$

$$\tilde{T}(|t|) = \frac{\hat{T}(|t|)}{N_{hs}} \sum_{i=1}^{N_{hs}} e^{-i\vec{\Delta}\cdot\vec{b}}$$

$$\frac{\mathrm{d}\sigma_{\mathrm{inc.}}}{\mathrm{d}t} \propto \left\langle \left| \tilde{T}(\vec{\Delta}) \right|^2 \right\rangle - \left| \left\langle \tilde{T}(\vec{\Delta}) \right\rangle \right|^2$$

First moment: $\left\langle \tilde{T}(|t|) \right\rangle = \hat{T} e^{-B_{qc}|t|/2}$

Second moment:

$$\left\langle \left| \tilde{T}(|t|) \right|^2 \right\rangle = \frac{\hat{T}^2}{N_{hs}^2} \sum_{i=1}^{N_{hs}} \sum_{j=1}^{N_{hs}} \left\langle e^{-i\vec{\Delta}\cdot(\vec{b}_i - \vec{b}_j)} \right\rangle = \frac{\hat{T}^2}{N_{hs}^2} \left[N_{hs} + N_{hs}(N_{hs}-1) \left\langle e^{-i\vec{\Delta}\cdot\vec{b}_i} \right\rangle \left\langle e^{-i\vec{\Delta}\cdot\vec{b}_j} \right\rangle \right]$$

$$= \frac{\hat{T}}{N_{hs}} \left(1 + (N_{hs}-1) e^{-B_{qc}|t|} \right)$$

Variance: $\mathrm{Var}_{\mathrm{geom.}} = \frac{\hat{T}^2}{N_{hs}} \left(1 - e^{-Bqc|t|} \right)$ Finite when $N_{hs} = 1$

Analytical calculation of the cross sections

First moment:

$$\phi(|t|) \equiv \left\langle e^{-i\vec{\Delta}\cdot\vec{b}} \right\rangle = \int \mathrm{d}^2\vec{b} T_c(\vec{b}) e^{-i\vec{b}\vec{\Delta}} = e^{-B_{qc}|t|/2}$$

Assuming Gaussian centres

$$\left\langle \tilde{T}(|t|) \right\rangle = \frac{\hat{T}(|t|)}{N_{hs}} \sum_{i=1}^{N_{hs}} \left\langle e^{i\vec{\Delta}\cdot\vec{b}} \right\rangle = \hat{T} e^{-B_{qc}|t|/2}$$

Assuming independent hotspots

Shift such that center-of-mass is at $\vec{0}$:

$$\vec{b}_i' = \vec{b}_i - \left\langle \vec{b} \right\rangle = \vec{b}_i - \frac{1}{N_{hs}} \sum_{i=1}^{N_{hs}} \vec{b}_i = \vec{b}_i \left(1 - \frac{1}{N_{hs}} \right) - \frac{1}{N_{hs}} \sum_{k \neq i} \vec{b}_k$$

$$F(|t|) \equiv \left\langle e^{-i\vec{\Delta}\cdot\vec{b}'} \right\rangle = \left\langle e^{-i\frac{N_{hs}-1}{N_{hs}}\vec{\Delta}\cdot\vec{b}_i} \right\rangle \prod_{k \neq i} \left\langle e^{-\frac{1}{N_{hs}}\vec{\Delta}\cdot\vec{b}_k} \right\rangle$$

$$= \phi\left(\frac{N_{hs}-1}{N_{hs}} \Delta \right) \left[\phi\left(\frac{\Delta}{N_{hs}} \right) \right]^{N_{hs}-1} = \exp\left[-\frac{1}{2} B_{qc} |t| \frac{N_{hs}-1}{N_{hs}} \right]$$

$$\left\langle \tilde{T}'(\Delta) \right\rangle = F \hat{T}$$

Analytical calculation of the cross sections

IPnonsat (leading twist):

$$F(|t|) = \exp\left[-\frac{1}{2}B_{qc}|t|\frac{N_{hs}-1}{N_{hs}}\right]$$

$$\left\langle \tilde{T}'(\Delta) \right\rangle = F\hat{T}$$

$$\frac{\mathrm{d}\sigma_{\mathrm{coh.}}}{\mathrm{d}t} \propto \left| \left\langle \tilde{T}(\vec{\Delta}) \right\rangle \right|^2$$

$$\frac{\mathrm{d}\sigma_{\mathrm{inc.}}}{\mathrm{d}t} \propto \left\langle \left| \tilde{T}(\vec{\Delta}) \right|^2 \right\rangle - \left| \left\langle \tilde{T}(\vec{\Delta}) \right\rangle \right|^2$$

$$\mathrm{Var}_{\mathrm{geom.}}[T_p] = \frac{\hat{T}^2}{N_{hs}}\left[1 + (N_{hs}-1)e^{-B_{qc}|t|}\right] - \hat{T}^2 F^2(|t|)$$

$\rightarrow 0$ when $N_{hs} = 1$, and $N_{hs} \rightarrow \infty$, or for $|t| \rightarrow 0$
$\rightarrow \hat{T}/N_{hs}$ when $|t| \rightarrow \infty$

Adding saturation scale fluctuations, each hotspot multiplied by ξ_i from log-normal distr.

$$\mathrm{Var}_{\mathrm{tot.}} = \mathrm{Var}_{\mathrm{geom.}}[T_p] + \left(e^{4\lambda_g^2\sigma_S^2} - 1\right)\frac{\hat{T}^2}{N_{hs}}$$

$$\langle \xi \rangle = 1$$

$$\left\langle \xi^2 \right\rangle = \exp(4\lambda_g^2\sigma_S^2)$$

The Hotspot Shape

Results from Lattice QCD,
M. Loan and Y. Ying, Prog. Theor. Phys. 116, 169 (2006) [hep-lat/0603030].:

A glue ball with mass $m_{0++} = 1.680 \pm 0.046$ is described by a wave function with radial solution:

$$R(r) = \exp\left[-A\left(\frac{r}{\lambda}\right)^{B}\right],$$

$$A = 0.883 \pm 0.045,\ B = 1.028 \pm 0.132 \approx 1$$

Laplacian!

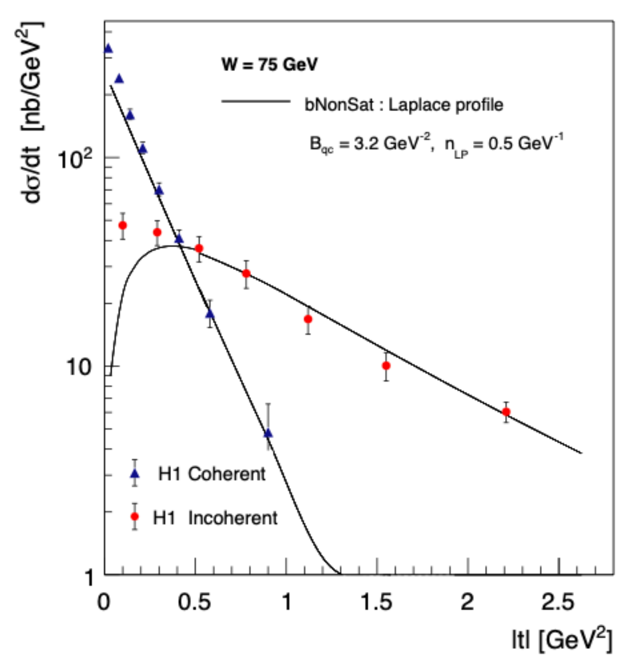

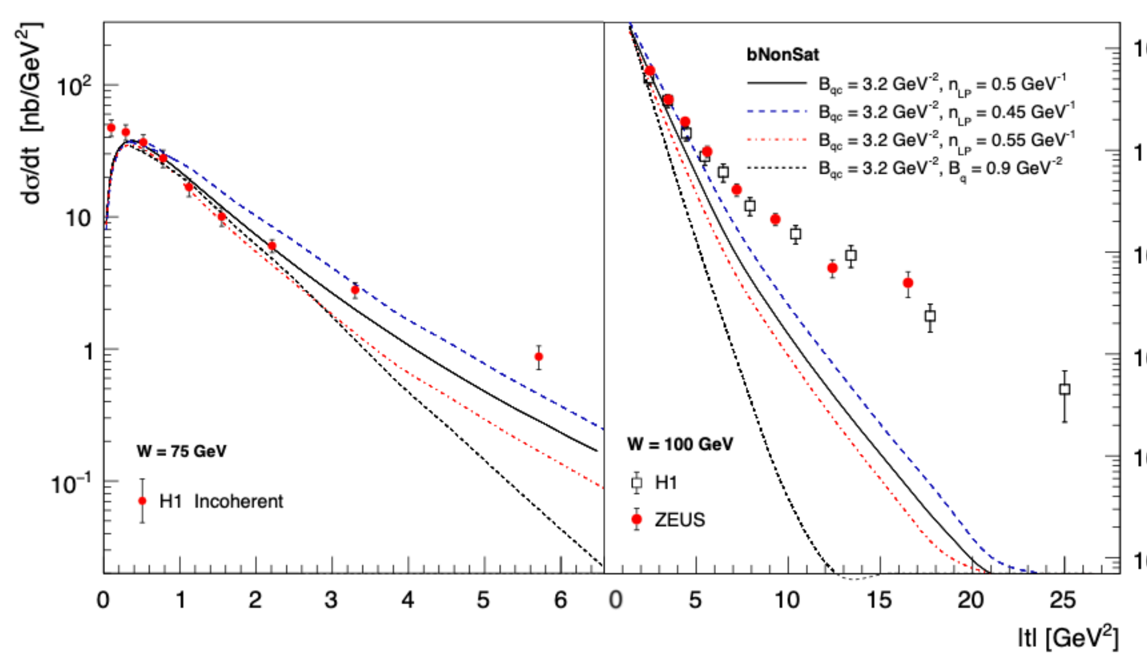

The Hotspot Shape

Topological structure of the entanglement radius of Yang-Mills flux tubes
Rocco Amorosso, Sergey Syritsyn, Raju Venugopalan, e-Print: 2603.10255 [hep-lat
R. Amorosso, S. Syritsyn, and R. Venugopalan, JHEP 12, 177 (2024)

Calculating fluxtube geometry from entanglement entropy:

“Gaussian peak centred at $x = -\xi_0$ and an exponential decay $\propto e^{-x/\lambda}$in its tails – this decay length $\lambda/\sqrt{\sigma_0} = 0.223(15)$ is consistent with both the inverse glueball mass and the intrinsic width of the flux tube”

$$\sigma_0 \sim 1 \text{ GeV/fm} \Rightarrow \lambda \sim 0.5 \text{ fm}$$

Massimo D’Elia, A. Di Giacomo, E. Meggiolaro, Phys.Lett.B 408 (1997) 315-319

Quenched YM results: $\lambda = 0.22 \pm 0.01 \pm 0.02 \text{ fm}$

The Hotspot Shape

Topological structure of the entanglement radius of Yang-Mills flux tubes
Rocco Amorosso, Sergey Syritsyn, Raju Venugopalan, e-Print: 2603.10255 [hep-lat
R. Amorosso, S. Syritsyn, and R. Venugopalan, JHEP 12, 177 (2024)

Calculating fluxtube geometry from entanglement entropy:

"Gaussian peak centred at $x = -\xi_0$ and an exponential decay $\propto e^{-x/\lambda}$ in its tails – this decay length $\lambda/\sqrt{\sigma_0} = 0.223(15)$ is consistent with both the inverse glueball mass and the intrinsic width of the flux tube"

$$\sigma_0 \sim 1 \text{ GeV/fm} \Rightarrow \lambda \sim 0.5 \text{ fm}$$

$$T_{hs}(b) = \int \mathrm{d}b' T_G(b - b') T_{\text{Lapl.}}(b')$$

$$T_G = \frac{1}{2\pi B_{hs}} e^{-\frac{b^2}{2B_{hs}}} \qquad T_{\text{Lapl.}}(b) = \frac{1}{2\pi\lambda^2} K_0\left(\frac{b}{\lambda}\right)$$

$$\hat{T}(|t|) = \frac{e^{-B_{hs}|t|/2}}{1 + \lambda^2|t|}$$

3 Models for energy dependence:

1. $B_{qc}(x_{I\!P}) = B_{qc0} + 2\alpha' \log(x_0/x_{I\!P})$

2. Model 1 and $B_{hs}(x_{I\!P}) = B_{hs0} + 2\beta' \log(x_0/x_{I\!P})$

3. Model 1 and $N_{hs}(x_{I\!P}) = N_{hs0}(x_0/x_{I\!P})^{\delta_N}$

Results

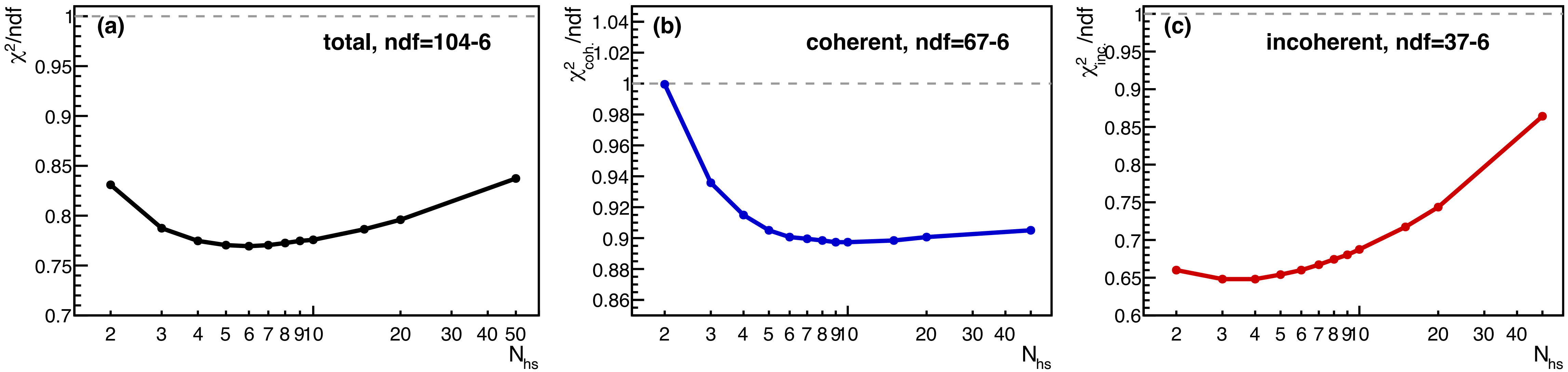

Fitted 6 parameters: $B_{qc0}, B_{hs}, \lambda, \sigma_S, \alpha'$, and normalisation.

Very good fit to the measurements (all errors treated as uncorrelated)

One unit of χ^2 within $4 \leq N_{hs} \leq 10$

Coherent best fit for $N_{hs} = 9$ (can describe the data with $N_{hs} \to \infty$), not sensitive to N_{hs}

Incoherent data prefers $N_{hs} = 3 - 4$

S. Chekanov et al. (ZEUS), Eur. Phys. J. C 26, 389 (2003), arXiv:hep-ex/0205081.
A. Aktas et al. (H1), Phys. Lett. B 568, 205 (2003), arXiv:hep-ex/0306013.
A. Aktas et al. (H1), Eur. Phys. J. C46, 585 (2006), arXiv:hep-ex/0510016.
S. Chekanov et al. (ZEUS), JHEP 05, 085, arXiv:0910.1235 .
C. Alexa et al. (H1), Eur. Phys. J. C73, 2466 (2013), arXiv:1304.5162.

Results

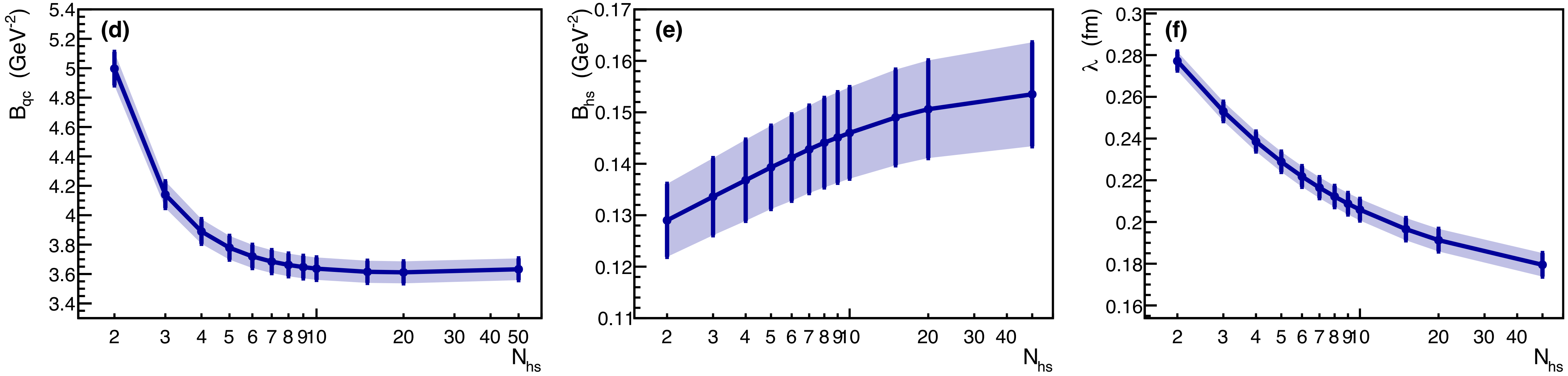

Within best fit range, $3.5 \leq B_{qc0} \leq 3.9\ \mathrm{GeV}^{-2}$, consistent with the MS model

Hotspot geometry:

$$0.137(8) \leq B_{hs} \leq 0.146(9)\ \mathrm{GeV}^{-2}, \qquad 0.206(5) \leq \lambda \leq 0.239(5)\ \mathrm{fm}$$

Perturbative Gaussian core of size $\sqrt{2B_{hs}} = 0.105\ \mathrm{fm}$ surrounded by a exponential halo with penetration depth $\lambda = 0.22\ \mathrm{fm}$.

Consistent with the lattice prediction of for the exponential tail in vacuum and a factor of 2 above the glue ball prediction (depending on string tension).

Results

$$\sigma_S \propto \log(N_{hs})$$

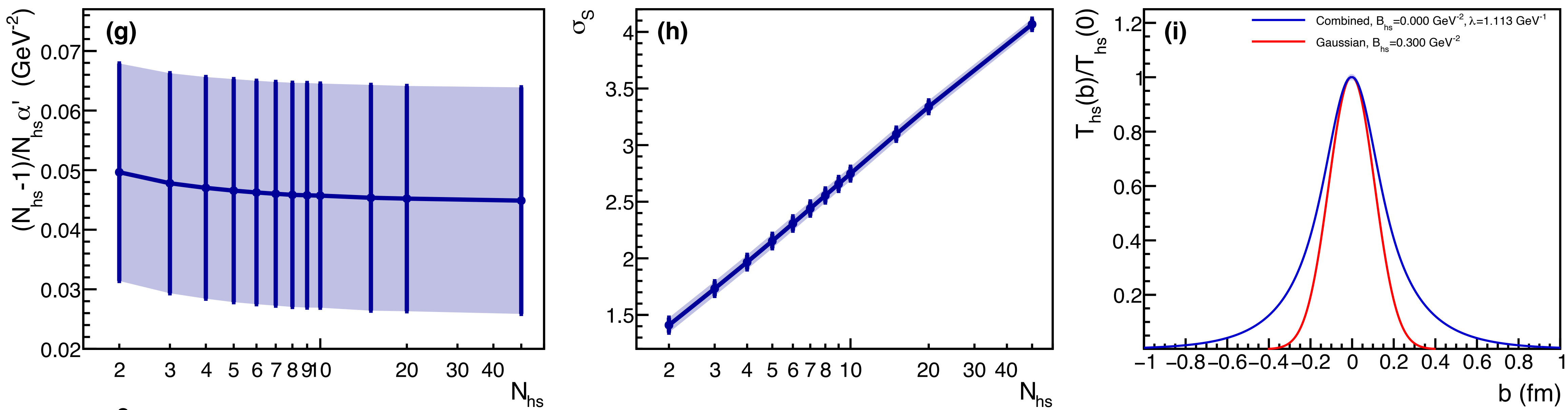

$$\alpha' = \frac{\partial^2 \sigma}{\partial W^2 \partial t} \qquad F(|t|) = \exp\left[-\frac{1}{2} B_{qc} |t| \frac{N_{hs} - 1}{N_{hs}}\right]$$

$$B_{qc}(x_{I\!P}) = B_{qc0} + 2\alpha' \log(x_0/x_{I\!P})$$

$$\alpha'_{\text{eff}} = \frac{N_{hs} - 1}{N_{hs}} \alpha' = 0.046(19)\ \text{GeV}^{-2},$$

consistent with running coupling BFKL predictions, Lotter (arXiv:hep-ph/9705288)
$\alpha' \approx 0.05\ \text{GeV}^{-2}$.

ZEUS: $\alpha' = 0.114 \pm 0.018^{+0.008}_{-0.015}\ \text{GeV}^{-2}$, H1: $\alpha' = 0.164 \pm 0.028 \pm 0.030\ \text{GeV}^{-2}$

	Fit 1	Fit 2 $B_{hs}(x_{\mathbb{P}})$	Fit 3 $N_{hs}(x_{\mathbb{P}})$
B_{q0} (GeV^{-2})	3.89(8)	3.94(9)	3.71(15)
B_{hs0} (GeV^{-2})	0.137(8)	0.169(21)	0.141(9)
λ (fm)	0.239(5)	0.232(6)	0.232(8)
σ_S	1.967(64)	1.940(68)	2.05(11)
α' (GeV^{-2})	0.063(25)	0.038(28)	0.024(38)
β' (GeV^{-2})		0.018(10)	
δ_N			0.068(66)
$\alpha'_{\text{eff.}}$	0.047(19)	0.047(24)	0.043 − 0.049
χ^2/ndf	75.92/98	73.94/97	75.40/97
$\chi^2_{\text{coh.}}/\text{ndf}_{\text{coh.}}$	55.81/61	55.41/60	55.34/60
$\chi^2_{\text{inc.}}/\text{ndf}_{\text{inc.}}$	20.09/31	18.61/30	20.02/30

$$\alpha'_{\text{eff.}}(1) = \frac{N_{hs}-1}{N_{hs}}\alpha' \qquad \alpha'_{\text{eff.}}(2) = \frac{N_{hs}-1}{N_{hs}}\alpha' + \beta' \qquad \alpha'_{\text{eff.}}(3) = \frac{N_{hs}-1}{N_{hs}}\alpha' + \frac{B_{qc0}\delta_N}{2N_{hs}}$$

	Fit 1	Fit 2 $B_{hs}(x_{I\!P})$	Fit 3 $N_{hs}(x_{I\!P})$
B_{q0} (GeV^{-2})	3.89(8)	3.94(9)	3.71(15)
B_{hs0} (GeV^{-2})	0.137(8)	0.169(21)	0.141(9)
λ (fm)	0.239(5)	0.232(6)	0.232(8)
σ_S	1.967(64)	1.940(68)	2.05(11)
α' (GeV^{-2})	0.063(25)	0.038(28)	0.024(38)
β' (GeV^{-2})		0.018(10)	
δ_N			0.068(66)
$\alpha'_{\text{eff.}}$	0.047(19)	0.047(24)	0.043 – 0.049
χ^2/ndf	75.92/98	73.94/97	75.40/97
$\chi^2_{\text{coh.}}/\text{ndf}_{\text{coh.}}$	55.81/61	55.41/60	55.34/60
$\chi^2_{\text{inc.}}/\text{ndf}_{\text{inc.}}$	20.09/31	18.61/30	20.02/30

Fit 1 Correlations

	Bqc	**Bhs**	**lambda**	**log(ng)**	**sigma_Q**	**alpha'**
Bqc	1.000					
Bhs	**0.469**	1.000				
lambda	**-0.671**	**-0.742**	1.000			
log(ng)	0.182	-0.254	**0.431**	1.000		
sigma_Qs	**-0.690**	-0.247	**0.681**	-0.015	1.000	
alpha'	-0.058	0.001	0.008	-0.065	0.053	1.000

	Fit 1	Fit 2 $B_{hs}(x_{\mathbb{P}})$	Fit 3 $N_{hs}(x_{\mathbb{P}})$
B_{q0} (GeV^{-2})	3.89(8)	3.94(9)	3.71(15)
B_{hs0} (GeV^{-2})	0.137(8)	0.169(21)	0.141(9)
λ (fm)	0.239(5)	0.232(6)	0.232(8)
σ_S	1.967(64)	1.940(68)	2.05(11)
α' (GeV^{-2})	0.063(25)	0.038(28)	0.024(38)
β' (GeV^{-2})		0.018(10)	
δ_N			0.068(66)
$\alpha'_{\text{eff.}}$	0.047(19)	0.047(24)	0.043 – 0.049
χ^2/ndf	75.92/98	73.94/97	75.40/97
$\chi^2_{\text{coh.}}/\text{ndf}_{\text{coh.}}$	55.81/61	55.41/60	55.34/60
$\chi^2_{\text{inc.}}/\text{ndf}_{\text{inc.}}$	20.09/31	18.61/30	20.02/30

$$\alpha'_{\text{eff.}}(2) = \frac{N_{hs}-1}{N_{hs}}\alpha' + \beta'$$

Fit 2 correlations

	Bqc	**Bhs**	**lambda**	**log(ng)**	**sigma_Q**	**alpha'**	**beta'**
Bqc	1.000						
Bhs	0.471	1.000					
lambda	**-0.693**	**-0.802**	1.000				
log(ng)	0.108	-0.313	0.467	1.000			
sigma_Qs	**-0.717**	-0.329	**0.679**	0.041	1.000		
alpha'	-0.216	-0.453	0.321	0.064	0.171	1.000	
beta'	0.347	**0.936**	**-0.651**	-0.249	-0.261	**-0.483**	1.000

	Fit 1	Fit 2 $B_{hs}(x_{I\!P})$	Fit 3 $N_{hs}(x_{I\!P})$
B_{q0} (GeV^{-2})	3.89(8)	3.94(9)	3.71(15)
B_{hs0} (GeV^{-2})	0.137(8)	0.169(21)	0.141(9)
λ (fm)	0.239(5)	0.232(6)	0.232(8)
σ_S	1.967(64)	1.940(68)	2.05(11)
α' (GeV^{-2})	0.063(25)	0.038(28)	0.024(38)
β' (GeV^{-2})		0.018(10)	
δ_N			0.068(66)
$\alpha'_{\mathrm{eff.}}$	0.047(19)	0.047(24)	0.043 – 0.049
χ^2/ndf	75.92/98	73.94/97	75.40/97
$\chi^2_{\mathrm{coh.}}/\mathrm{ndf}_{\mathrm{coh.}}$	55.81/61	55.41/60	55.34/60
$\chi^2_{\mathrm{inc.}}/\mathrm{ndf}_{\mathrm{inc.}}$	20.09/31	18.61/30	20.02/30

$$\alpha'_{\mathrm{eff.}}(3) = \frac{N_{hs}-1}{N_{hs}}\alpha' + \frac{B_{qc0}\delta_N}{2N_{hs}}$$

Fit 3 correlations

	Bqc	**Bhs**	**lambda_**	**log(ng)**	**sigma_Q**	**alpha'**	**delta_N**
Bqc	1.000						
Bhs	0.476	1.000					
lambda	**-0.693**	**-0.739**	1.000				
log(ng)	0.211	-0.231	0.381	1.000			
sigma_Qs	**-0.621**	-0.391	**0.646**	-0.010	1.000		
alpha'	-0.083	-0.248	0.077	-0.030	0.462	1.000	
delta_N	0.045	0.304	-0.082	-0.018	**-0.543**	**-0.796**	1.000

Results

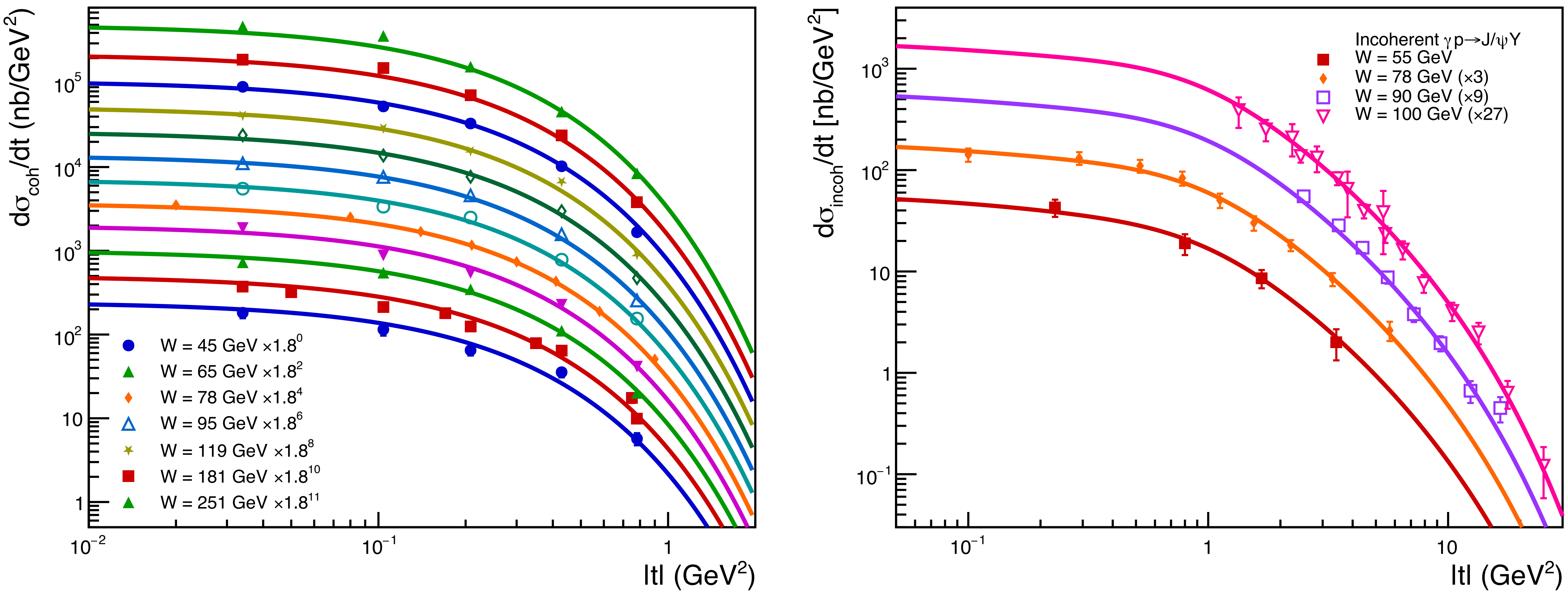

S. Chekanov et al. (ZEUS), Eur. Phys. J. C 26, 389 (2003), arXiv:hep-ex/0205081.
A. Aktas et al. (H1), Phys. Lett. B 568, 205 (2003), arXiv:hep-ex/0306013.
A. Aktas et al. (H1), Eur. Phys. J. C46, 585 (2006), arXiv:hep-ex/0510016.
S. Chekanov et al. (ZEUS), JHEP 05, 085, arXiv:0910.1235 .
C. Alexa et al. (H1), Eur. Phys. J. C73, 2466 (2013), arXiv:1304.5162.

Conclusions and Outlook

Remarkably stable hotspot geometry, from several different models etc.
(We also tried a hotspot repulsion, which did not affect their geometry)
HERA data could not resolve any $x_{I\!P}$ dependence of the hotspots.

The emergent picture: The proton small-*x* proton consists of 3-4 hotspots with a hard Gaussian core of 0.105(2) fm, surrounded by an exponential halo of size 0.220(15) fm. These are frozen in $x_{I\!P}$.

Next steps:
Comprehensive dipole model fit to inclusive reduced cross section and exclusive data

Investigate hotspot correlations.

Extend the analytical calculation to nuclei and higher twists.

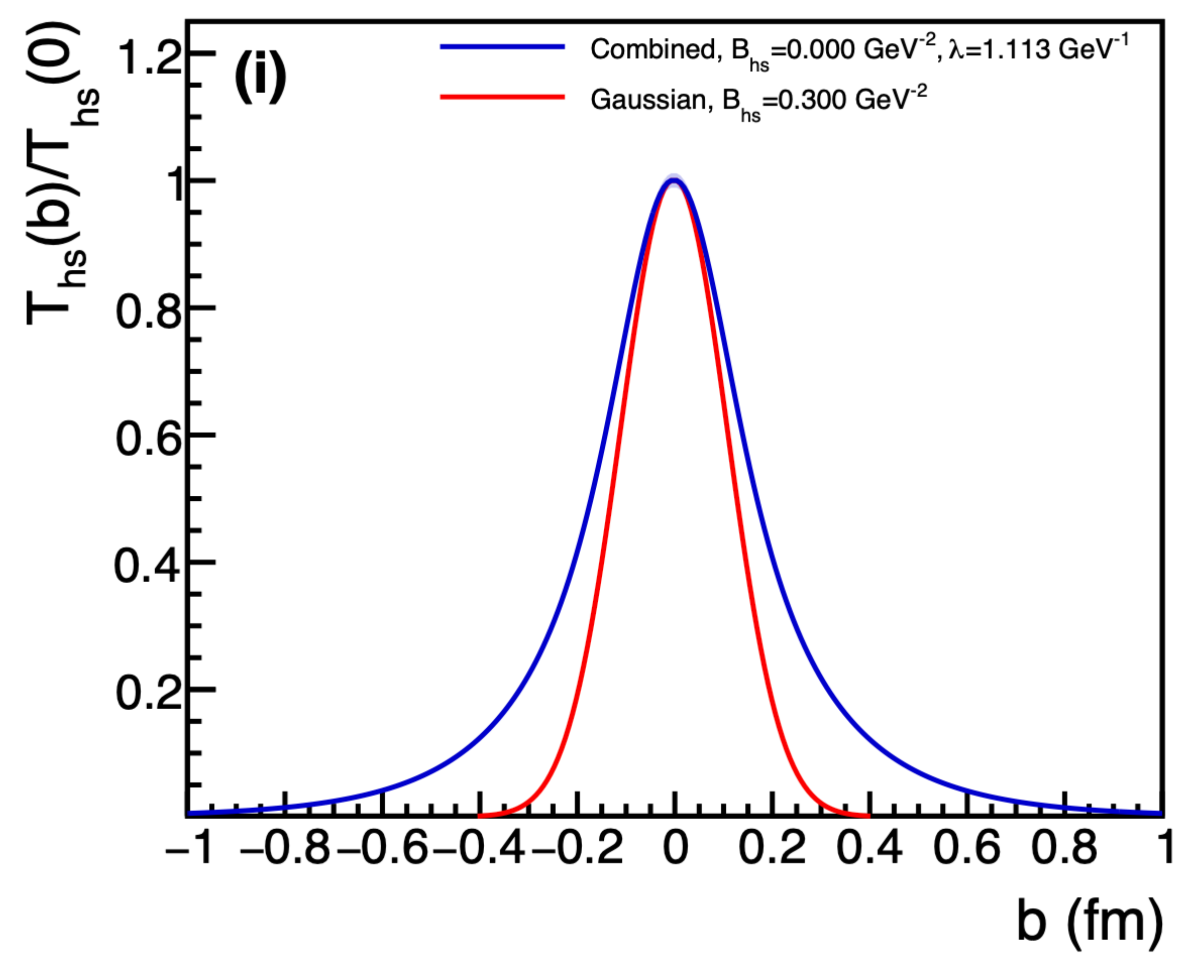

Conclusions and Outlook

Remarkably stable hotspot geometry, from several different models etc.
(We also tried a hotspot repulsion, which did not affect their geometry)
HERA data could not resolve any $x_{I\!P}$ dependence of the hotspots.

The emergent picture: The proton small-*x* proton consists of 3-4 hotspots with a hard Gaussian core of 0.105(2) fm, surrounded by an exponential halo of size 0.220(15) fm. These are frozen in $x_{I\!P}$.

Next steps:
Comprehensive dipole model fit to inclusive reduced cross section and exclusive data

Investigate hotspot correlations.

Extend the analytical calculation to nuclei and higher twists.